(2)

Annual Technical Report on ONR Grant N00014-92-J-1008 for a Period of Time: October 1, 1992-September 30, 1993

by

Michael V. Klibanov
Principal Investigator
Department of Mathematics
University of North Carolina at Charlotte
Charlotte, NC 28223
fma@@mvk@unccvm.uncc.edu

and

Semion Gutman
Subcontractor
Department of Mathematics
University of Oklahoma
Norman, OK 73019
sgutman@nsfuvax.math.uoknor.edu

Introduction. We have been working on the following issues:

1. Computations for 2-Dimensional and 3-Dimensional Inverse Scattering Problems (ISP) for the Helmholtz equation. Convergence analysis of our numerical method for this equation.

2. Globally convergent numerical methods for 3-D ISP.

3. Numerical method for phaseless 1-D ISP.

4. Mathematical model for light propagation in highly scattering media (interdisciplinary research effort).

Below we briefly describe these developments. They have been described in detail in references [4]-[6], [8]-[17].

1. Convergence Analysis and Computational Experiments for 2-D and 3-D ISPs for the Helmholtz Equation. See [4]-[6], [8] and [9].

Let Ω be a bounded domain in $\mathbb{R}^3$ with a dielectric function $1+\varepsilon(x)$, where $\varepsilon(x) \in L^\infty(\Omega)$ represents relative fluctuations of the dielectric function, $\varepsilon(x) = 0$ outside of Ω and $\varepsilon(x)$ is unknown inside of Ω. Without loss of generality we assume $\Omega \subset W$, where W is the ball of radius $\pi/2$ with the center at the origin. Let ∂W be the spherical boundary of W and S^2 be the unit sphere in $\mathbb{R}^3$. If $\nu \in S^2$, then $e^{ik<x,\,\nu>}$ is the scalar incident planar wave of the frequency k propagating in the direction of the vector ν. Here $<\cdot,\ \cdot>$ is the inner product in $\mathbb{R}^3$. Let $u(x,\nu)$ be the solution of the forward scattering problem

$$\Delta u + k^2(1+\varepsilon(x))u = 0 \tag{1.1}$$

$$u(x,\nu) = e^{ik<x,\nu>} + \tilde{u}(x,\nu) \tag{1.2}$$

plus Sommerfield radiation conditions.

The ISP Statement. Let $k = \text{const.} > 0$ be fixed. Determine the function $\varepsilon(x)$ in (1.1)

assuming that the measurement function $\varphi(x, \nu)$, $\nu \in S^2$, $x \in \partial W$ is given and the function $u(x, \nu)$ satisfies

$$u|_{\partial W} = \varphi(x, \nu), \quad \forall \nu \in S^2 \tag{1.3}$$

In [14] we proposed a quasi-Newton method for this problem. During this year our developments in this direction were the following:

a) We derived a completely rigorous proof of convergence of our original algorithm [4], [6].

b) We tested complicated geometries, rather than just cylinders as it was earlier [9]. Our original code required certain changes to do this.

c) The major effort was devoted to solution of a challenging 3-D, rather than 2-D ISP. (see below)

In our algorithm we represent $\varepsilon(x)$ in the form of a finite Fourier series,

$$\varepsilon(x) = \sum_{|n| \le N} a_n e^{i<n, x>}, \tag{1.4}$$

where N is a fixed integer, $N \le \frac{2k}{\sqrt{3}}$ in 3-D case, and $N \le \sqrt{2}k$ in 2-D case. Hence we cut high frequency harmonics of ε. The algorithm consists in an iterative search of Fourier coefficients a_n.

Test #1. [9] As an example of a complex geometry consider $\varepsilon(x)$ which is non-zero inside of a non-symmetric cross and a cylinder, see Fig. 1a. That is

$$\varepsilon(x) = \begin{cases} 0.01, \text{ for } \sqrt{(x_1 + 0.2\pi)^2 + (x_2 + 0.2\pi)^2} < 0.15\pi \\ 0.01, \text{ for } 0.6 < x_1 < 1 \text{ and } 0.2 < x_2 < 1.3 \\ 0.01, \text{ for } 0.2 < x_1 < 1.3 \text{ and } 0.6 < x_2 < 1 \\ 0, \qquad\qquad\qquad \text{otherwise} \end{cases}$$

We have also included twelve randomly distributed spikes in order to see how random fluctuations might affect our solution. Results of our computations at $N = 10$ are displayed on Figs. 1b-1d.

Fig. 1b represents the 3-D view of the computed ε; the spikes are removed. Figs. 1c and 1d display views from the "top" or real and computed ε respectively. Computations were made on NAVY CRAY-Y/MP. CPU time was 2 minutes.

In the test #3 we present solution of a 3-D ISP, which was obtained, *for the first time* (cf. [2], where computations of a non-symmetric 3-D ISP was stated as a challenging problem). CPU time was 30 minutes, at $N = 7$, which is much less than would be required by other currently available methods.

Test #3. 3-D ISP.

In order to avoid solving of 3-D forward problem, for data simulation we have taken the ball,

$$\varepsilon(x) = \begin{cases} 0.02, & \text{for } |x| < 1.26 \\ 0, & \text{otherwise} \end{cases}$$

Forward problem (1.1), (1.2) admits an explicit solution on this case. However, we have never assumed, whatsoever, any kind of symmetry when inverse problem was being solved.

In order to reduce dramatically the CPU time, we have made a crucial modification of our original algorithm. Namely instead of using $(2N+1)^3$ different directions ν we employed some "basic" vectors ν. In order to get data for other needed directions we applied a special interpolation procedure using the fact that other ν-s are sufficiently close with basic ones. Thus this procedure allowed us to use 300 "basic" directions ν instead of $(2 \cdot 7+1)^3 = 3{,}375$ as it would be the case in [4], [5].

Figs. 2a, 2b represent cross-section of real $\varepsilon(x)$ by two different planes at the distance h from the center Figs. 2c, 2d display corresponding computed ε. Finally on Fig. 2e we present cross-section of tested (dashed line) and computed (solid line) $\varepsilon(x)$ by a straight line through the center. Work on an improvement of this result is

currently in progress.

2. Globally Convergent Numerical Methods for Hyperbolic 3-D ISP. [8], [11], [12].

This is an entirely new and promising direction of the research of numerical methods for 3-D ISPs. We hope that these results will lead us to effective working numerical schemes. There are two major advantages of these methods as compared with the method for Helmholtz equation: (i) These are "global", rather than "local" methods. That is the basis of convergence is just an arbitrary fixed compact set, rather than a "small" ball (in certain Banach space).

(ii) These are "single", rather than many-source methods. That is we consider non-overdetermined problem with just a single source position.

Single source problems are of much less computations complexity than many-source problems since they deal volumes of data which are of the order of a magnitude(s) less than in the case of many sources. The price for these advantages is two fold: (a) theory of these methods is much more sophisticated; (b) single-source problems are less informative.

The main tool in this direction is a deep modification of the method of Carleman estimates [13]. As to informativeness issue, the idea is to work with the data obtained from different sources by a step-by-step procedure, rather than working with many sources simultaneously. In this case one would improve the required image step-by-step and CPU time will be added, rather than mutliplied. Finally, one would deal with a much less number of sources, which, in principle, should decrease experimental complexity.

Let $T = \text{constant} > 0$, function $a(x) \in C^2(\mathbf{R}^3)$ and function $u(x, t)$ is solution of the Cauchy problem

$$u_{tt} = \Delta u + a(x)u, \text{ in } R^3_T = \mathbf{R}^3 \times (0, T)$$

$$u|_{t=0} = 0, \quad u_t|_{t=0} = \delta(x) \tag{2.1}$$

Consider cylinder $CL = \{x_1^2 + x_2^2 < r_0^2\}$, with the boundary ω where $r_0 = \text{constant} > 0$. Let $R = \text{const.}$, $R > r_0$, and $\Omega = \{|x| < R\} \setminus \{CL\}$.

The ISP statement. Determine function $a(x)$ inside of the domain Ω assuming that $a(x)$ is given inside of CL and the following function $\varphi(x, t)$ is given as well

$$u|_\omega = \varphi(x, t), \quad (x, t) \in \omega \times (0, T) \tag{2.2}$$

In [8], [11] we constructed a uniformly strictly convex cost functional for this ISP. Thus *global* convergence of a number of numerical methods was guaranteed. By the method [8], [11] one determines a finite number of Fourier coefficients of a function associated with the wave field $u(x, t)$. A more challenging and complicated problem, however, consists in determining of a finite number of Fourier harmonics of the unknown coefficient $a(x)$ itself. During the Spring, Summer and Fall of 1993 we have been actively working on development of such a numerical scheme. Now this method has been finally derived [12]. Thus algorithm combines our idea of quasi-reversibility method [14] with the method of [8], [11].

3. Numerical Method for Phaseless 1-D ISP. [17].

In the classical formulation of ISP for 1-D Schrödinger equation, one has to determine unknown potential $V(x)$ from the reflection coefficient $R(k)$ [3]. In many important applications, however, only the amplitude $|R(k)|^2$ can be measured. Let

$$A = \{V \in L^\infty(\mathbf{R}) \cap L_2^1(\mathbf{R}); \ V \text{ is real valued}, V(x) \equiv 0 \text{ for } x < 0\}$$

Here $L_2^1(\mathbf{R})$ is the weighted L^1 space

$$L_2^1(\mathbf{R}) = \{f: \int_{-\infty}^{\infty} (f(x))(1+x^2)dx < \infty\}$$

The time-reduced Schrödinger equation

$$\varphi'' + (k^2 - V(x))\varphi = 0, \quad -\infty < x < \infty \tag{3.1}$$

then has solutions

$$\begin{aligned} \Psi_1(x, k) &= e^{ikx} + R_-(k)e^{-ikx}, \quad x < 0 \\ &\sim T(k)e^{ikx}, \quad x \to +\infty \\ \Psi_2(x, k) &= T(k)e^{-ikx}, \quad x < 0 \\ &\sim e^{-ikx} + R_+(k)e^{ikx}, \ x \to +\infty \end{aligned} \tag{3.2}$$

The ISP Statement. Determine function $V \in A$ assuming that the reflection amplitude

$$r(k) = |R_-(k)|^2, \quad 0 \le k < \infty \tag{3.3}$$

is given.

Previously, we have proven uniqueness theorem for the problem (3.1)-(3.3). Recently, we have developed and tested a numerical method as well [17]. This method works for the case of a relatively small number of complex zeros of the function $R(k)$. Fig. 3 represents exact (solid line) and computed (dotted line) potentials $V(x)$. Computations were made by the algorithm [17]. Currently, we are also working on some modifications of the idea of [16].

4. Mathematical Model for Light Propagation in Highly Scattering Media. [10].

In the past several years different research groups have been using laser-based techniques to locate translucent objects in highly scattering media such as sea water, biological tissues, etc. [19], [20]. In the future, this technique might improve or even replace conventional X-ray tomography. The core of this kind of imaging, however, must be solving of full-scale 3-D ISPs, since the only hope to image internal structure of

inclusions with a fine resolution lies in applying of sophisticated inverse problems numerical methods. In particular, we hope that our numerical methods might be eventually applied to this challenging problem.

The first question which comes in mind, however, consists in the right mathematical model for this kind of processes. Because of our already developed algorithms, it would be desirable to have a hyperbolic equation, which would govern light propagation in highly scattering media. The light emitted from ultrafast laser pulses (~ 100 femtosecond duration) splits into three components in highly scattering media: ballistic, snake and diffuse [20]. The ballistic photons propagate along straight lines, just as X-rays. But intensity of the ballistic component is so small that it cannot be detected. So-called snake photons represent early arriving photons. They propagate slightly off straight lines and contain a good portion of information about inclusions. Fortunately, snake photons can be detected. Finally, diffuse photons represent the later portion of the signal. They have many scattering events before emission from the media and contain a very little information about inclusions. Overall, all photons, except of ballistic ones, experience random scattering inside of such kind of media.

Commonly, diffusion equation has been used for description of these processes [1]. The immediate shortcoming of diffusion equation, however, is its prediction that intensity of the light will be non-zero instantaneously everywhere. Besides, it was shown in [21] that diffusion equation cannot describe snake photons and that it is not valid for the thin media. After a long and careful analysis we suggested to use a hybrid wave-diffusion equation, which is equivalent with the telegraph equation [10]. In fact, wave-type equations were never used before in this kind of processes, although the telegraph equation was derived phenomenologically for heat propagation in the gas in [18, p. 865].

The telegraph equation for the intensity I(x, t) has the form

$$\frac{1}{c^2} I_{tt} + \frac{1}{D} I_t - \Delta I + \frac{1}{L^2} I = 0 \qquad (4.1)$$

We have also proposed special initial conditions which reflect the collimated nature of the initial laser beam propagating along the x_1-axis. These initial conditions are

$$I|_{t=0} = \delta(x) \qquad (4.2)$$

$$I_t|_{t=0} = -c^2 \frac{\partial}{\partial x_1} \delta(x) + \beta c \delta(x) \qquad (4.3)$$

Here the $c\beta\delta(x)$ term is included to keep intensity from being negative at $t \to \infty$, and β is a small positive number (we usually take $\beta = 0.03$). We can prove that this term provides a very small impact until time becomes very large.

In (4.1) c is the speed of light in the media, $D = c\ell_t/3$, is diffusion coefficient, ℓ_t is the mean free path of photons, $L^2 = \ell_t \ell_a/3$ and ℓ_a is the absorbtion length. In highly scattering media, such as biological media, usually $\ell_t = 1 \div 3$ mm and $\ell_a > 100$ mm.

We have tested validity of the equation (4.1) by comparison of the solution of the problem (4.1)-(4.3) with the experimental data for a large range of source-detector distances as well as for two source-detector configurations: (i) "face-to-face", that is for the case of transmitted light; (ii) perpendicular. Experimental data were obtained from Prof. R.R. Alfano (City College of CUNY, New York). Our data fitting results show that while for the thick media both telegraph and diffusion equation provide good fit with experimental curves, for thin media ($\leq 7\ell_t$) telegraph equation constantly provides much better fit.

Figures 4a, 4b, 5a, 5b, 6a and 6b represent comparison of the solutions of diffusion and telegraph equations (solid lines) with normalized experimental data (dashed lines). Face-to-face source-detector configuration was chosen in this particular set of experiments (we also have tested three more tests, and all of them provided similar results). Diffusion equation under consideration has the form

$$\frac{1}{D} I_t - \Delta I = 0$$

$$I|_{t=0} = c\delta(x)$$

Experimental data were arranged in such a way that influences of the boundaries of the media were negligible. Figs. labeled "a" and "b" represent fitting by the telegraph and diffusion equations respectively. In this set of experiments a medium with $\ell_t^0 = 0.55$mm and $\ell_a^0 = 405$ mm was taken. Here ℓ_t^0 and ℓ_a^0 are parameters ℓ_t and ℓ_a obtained by the fitting by diffusion equation for thick media. In using telegraph equation we discovered that parameters ℓ_t and ℓ_a should depend on the source-detector configuration. This is due to mixing up of wave and diffusion modes. Another explanation of this phenomenon is that in non-stationary kinetics these parameters should depend on photons momentum. This situation was predicted in [18, pp. 179-180].

Figs. 4a, 4b $|x|/\ell_t^0 = 18.18$, that is the media is thick. On Figs. 5a, b $|x|/\ell_t^0 = 7.27$; on Figs. 6a, b $|x|/\ell_t^0 = 5.45$, and $|x|/\ell_t^0 = 3.63$ on Figs. 7a, b. As we clearly see from these Figs. telegraph equation provides a much better fit for thin media with $|x|/\ell_t^0 \leq 7$.

One way of improvement of this model lies in working with convoluted data for I(x, t) rather than with I(x, t) itself. This is especially true for thin media because in fact streak camera convolutes the data, and it has 10 picosecond resolution only. Another way, might consist in working directly with more general transport equation. But new numerical methods for ISP need to be derived in this case, which might open a new direction of our research. Overall, we have undertaken a significant effort in theoretical physics working on this issue. Concurrently, we consider possibility of applying of our numerical methods for ISP to the problem of imaging of inclusions hidden in highly scattering media. Thus we should work with the telegraph equation, rather than just with the wave equation (3.1). Careful analysis of our algorithms shows that they can be modified for this case.

REFERENCES

1. S. Arridge, The forward and inverse problems in time-resolved infrared imaging, in *"Medical Optical Tomography: Functional Imaging and Monitoring"*, SPIE Institutes Series, Vol. 11, ed. G. Müller, (1993).

2. D. Colton and R. Kress, *Inverse Acoustics and Electromagnetic Scattering Theory*, Appl. Math. Sci., V. 93, Springer Verlag, New York, 1992.

3. P. Deiff and E. Trabowitz, Inverse scattering on the line, *Comm. Pure Appl. Math.*, 32 (1979), 121-551.

4. S. Gutman and M.V. Klibanov, Regularized quasi-Newton method for inverse scattering problems, *Int. J. Math. and Computer Modelling*, 18 (1993), 5-31.

5. S. Gutman and M.V. Klibanov, Quasi-Newton method for 3-dimensional inverse scattering problem, *Computational Acoustics*, V. 1, #2 (1993).

6. S. Gutman and M.V. Klibanov, Iterative method for multidimensional Inverse Scattering Problems at fixed frequencies, *Inverse Problems* (to appear).

7. G. Felcher and T. Russel, eds., Proceedings of the workshop on Methods of Analysis and Interpretation of Neutron Reflectivity Data, *Physica B*, Condensed Matter, 173 (1991).

8. M.V. Klibanov, S. Gutman and O.V. Ioussoupova, Multi-dimensional inverse scattering problems in random and deterministic media, *Proc. of SIAM Conf. of Wave Propagation Phenomena*, 1993, 302-310.

9. MV. Klibanov, S. Gutman, R. Barbour, J. Chang, J. Malinsky, and R.R. Alfano, Considerations of solutions of the inverse scattering problem for biomedical applications, *SPIE Proc.*, 1887 (1993), 77-95.

10. M.V. Klibanov, S. Gutman, F. Liu and R.R. Alfano, Wave-diffusion equation for pulse propagation in highly scattering media, *Proc. of the Conference "Advances in Optical Imaging and Photon Migration"*, 1993 (to appear).

11. M.V. Klibanov and O.V. Ioussoupova, Uniformly strictly convex cost functional for 3-D inverse scattering problem, *SIAM J. Math. Anal.*, to appear.

12. M.V. Klibanov and S. Gutman, Globally convergent numerical method for 3-Dimensional inverse scattering problem, *in preparation.*

13. M.V. Klibanov, Inverse problems and Carleman estimates, *Inverse Problems*, 8 (1992), 575-596.

14. M.V. Klibanov and J. Malinsky, Newton-Kantorovich method for 3-dimensional potential inverse scattering problem and stability of the hyperbolic Cauchy problem with time-dependent data, *Inverse Problems*, 7 (1991), 577-596.

15. M. Klibanov and S. Gutman, Mathematical algorithms for multidimensional inverse scattering problems in inhomogeneous medium, proposal for ONR funding, 1991.

16. M.V. Klibanov and P.E. Sacks, Phaseless inverse scattering and the phase problem in optics, *J. Math. Phys.* 33 (1992), 3813-3821.

17. M.V. Klibanov and P.E. Sacks, Use of partial knowledge of the potential in the phase problem of inverse scattering, *J. Computational Physics*, to appear.

18. P.M. Morse and H. Feshbach, *Methods of Theoretical Physics*, V. 1, McGraw-Hill, New York, 1953.

19. L. Wang, P. Ho, C. Liu, G. Zhang, and R. Alfano, Ballistic 2-D imaging through scattering walls using an ultrafast Kerr gate, *Science*, 253 (1991), 769-771.

20. K. Yoo, B. Das, and R. Alfano, Imaging of translucent object hidden in a highly scattering medium from the early portion of diffusive component of a transmitted ultrafast laser pulse, *Opt. Lett.*, 17 (1992), 958-960.

21. K. Yoo, F. Liu, and R. Alfano, When does the diffusion approximation fail to describe photon transport in random media, *Phys. Rev. Lett.*, 64 (1990), 2647-2650.

Figure Captions

Fig. 1a Test #1 3-D view on the test coefficient $\varepsilon(x)$.

Fig. 1b Test #1. 3-D view on the computed coefficient $\varepsilon(x)$.

Fig. 1c Test #1 View from the "top" on the test coefficient $\varepsilon(x)$.

Fig. 1d Test #1 View from the "top" on the computed coefficient $\varepsilon(x)$.

Fig. 2a Test #2 Cross-section of the test coefficient $\varepsilon(x)$ by the phase at $h = 0$ from the center.

Fig. 2b Test #2 Cross-section of the test coefficient $\varepsilon(x)$ by the plane of $h = 0.26$ from the center.

Fig. 2c Test #2 Cross-section of computed $\varepsilon(x)$ by the plane at $h = 0$ from the center.

Fig. 2d Test #2 Cross-section of computed $\varepsilon(x)$ by the plane at $h = 0.26$ from the center.

Fig. 2d Test #2 Cross-section of tested (dashed line) and computed (solid line) $\varepsilon(x)$ by a straight line through the center.

Fig. 3 Phaseless 1-D ISP. Exact (solid line) and computed (dashed line) potential $V(x)$.

Fig. 4a Telegraph equation solution (solid line) and experimental data (dashed line) for $|x|/\ell_t^0 = 18.18$.

Fig. 4b Diffusion equation solution (solid line) and experimental data (dashed line) for $|x|/\ell_t^0 = 18.18$.

Fig. 5a Telegraph equation solution (solid line) and experimental data (dashed line) for $|x|/\ell_t^0 = 7.27$.

Fig. 5b Diffusion equation solution (solid line) and experimental data (dashed line) for $|x|/\ell_t^0 = 7.27$.

Fig. 6a Telegraph equation solution (solid line) and experimental data (dashed line) for $|x|/\ell_t^0 = 5.45$.

Fig. 6b Diffusion equation solution (solid line) and experimental data (dashed line) for $|x|/\ell_t^0 = 5.45$.

Fig. 7a Telegraph equation solution (solid line) and experimental data (dashed line) for $|x|/\ell_t^0 = 3.63$.

Fig. 7b Diffusion equation solution (solid line) and experimental data (dashed line) for $|x|/\ell_t^0 = 3.63$.

Test coefficient

Fig. 1a

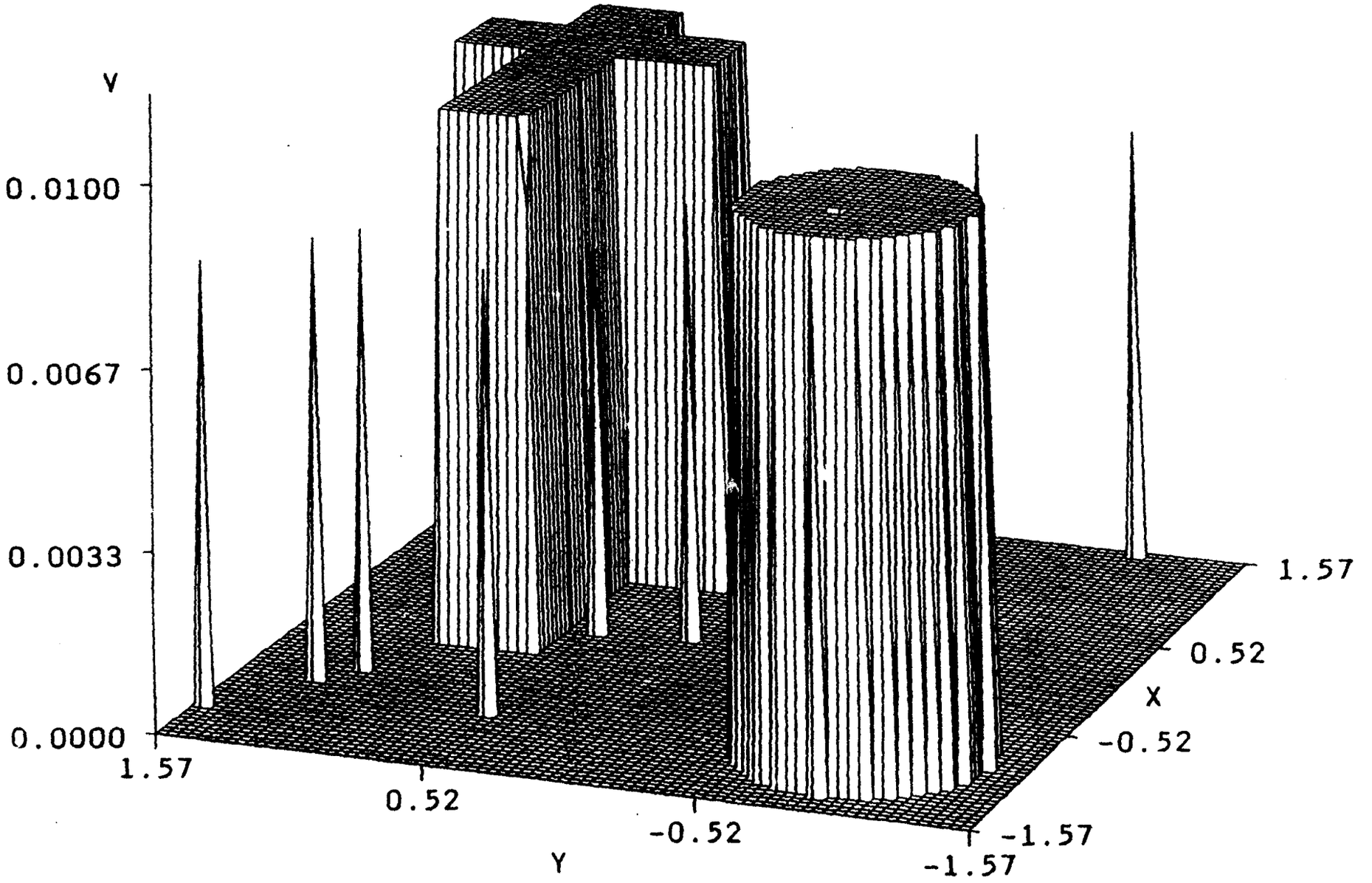

Estimated coefficient

Figure 1b

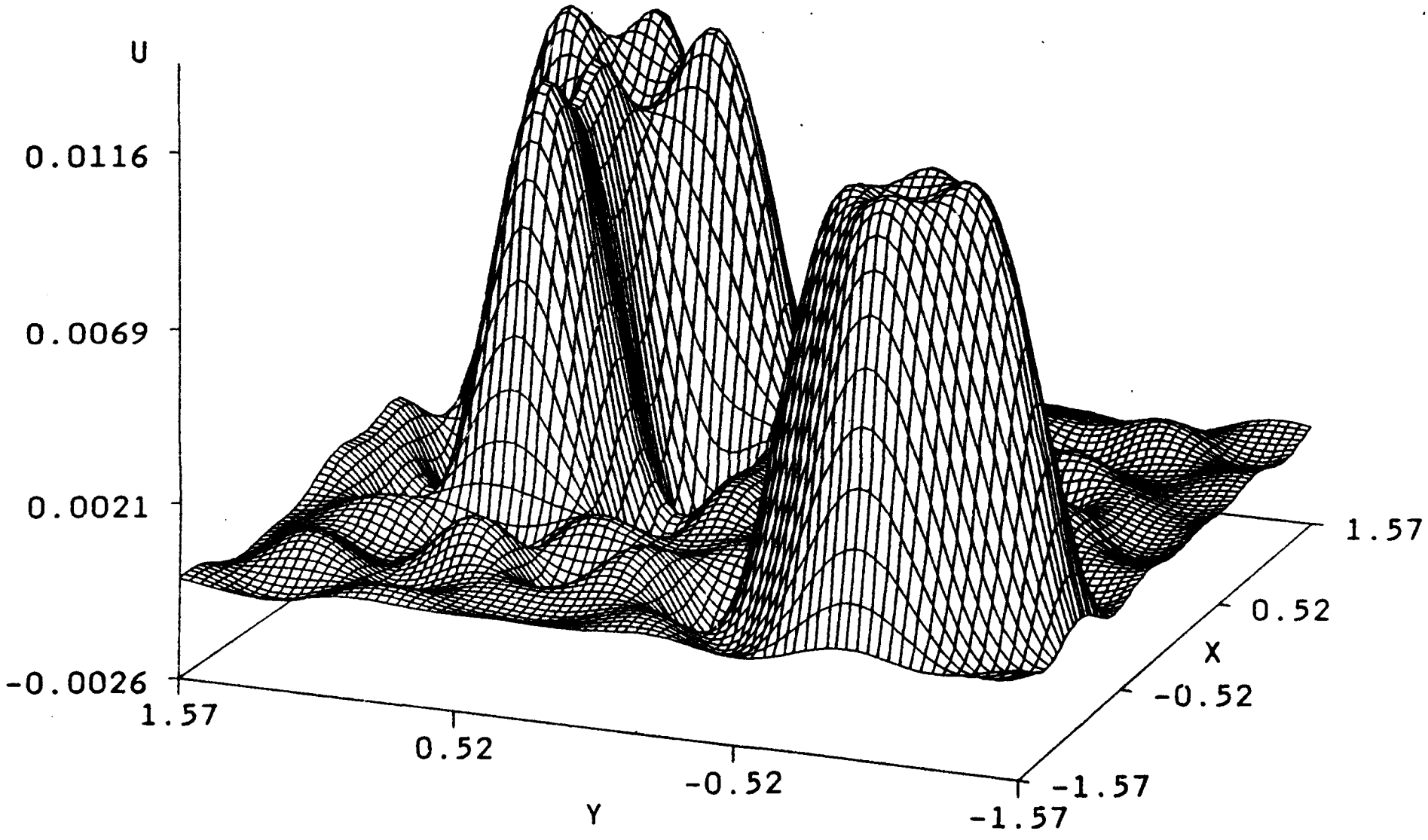

k = 10.1 m = 10

Test coefficient

Figure 1c

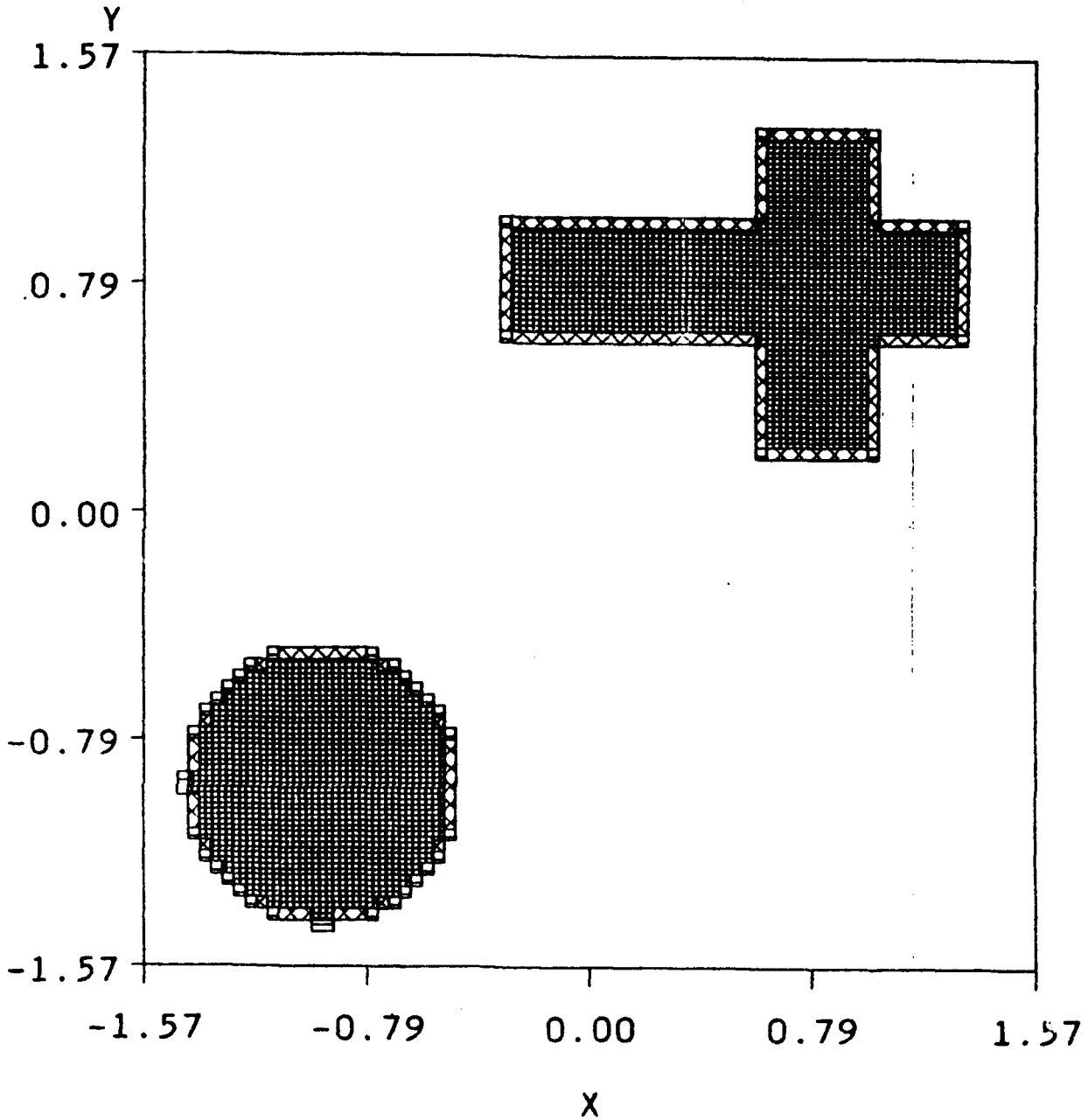

Estimated coefficient

Figure 1d

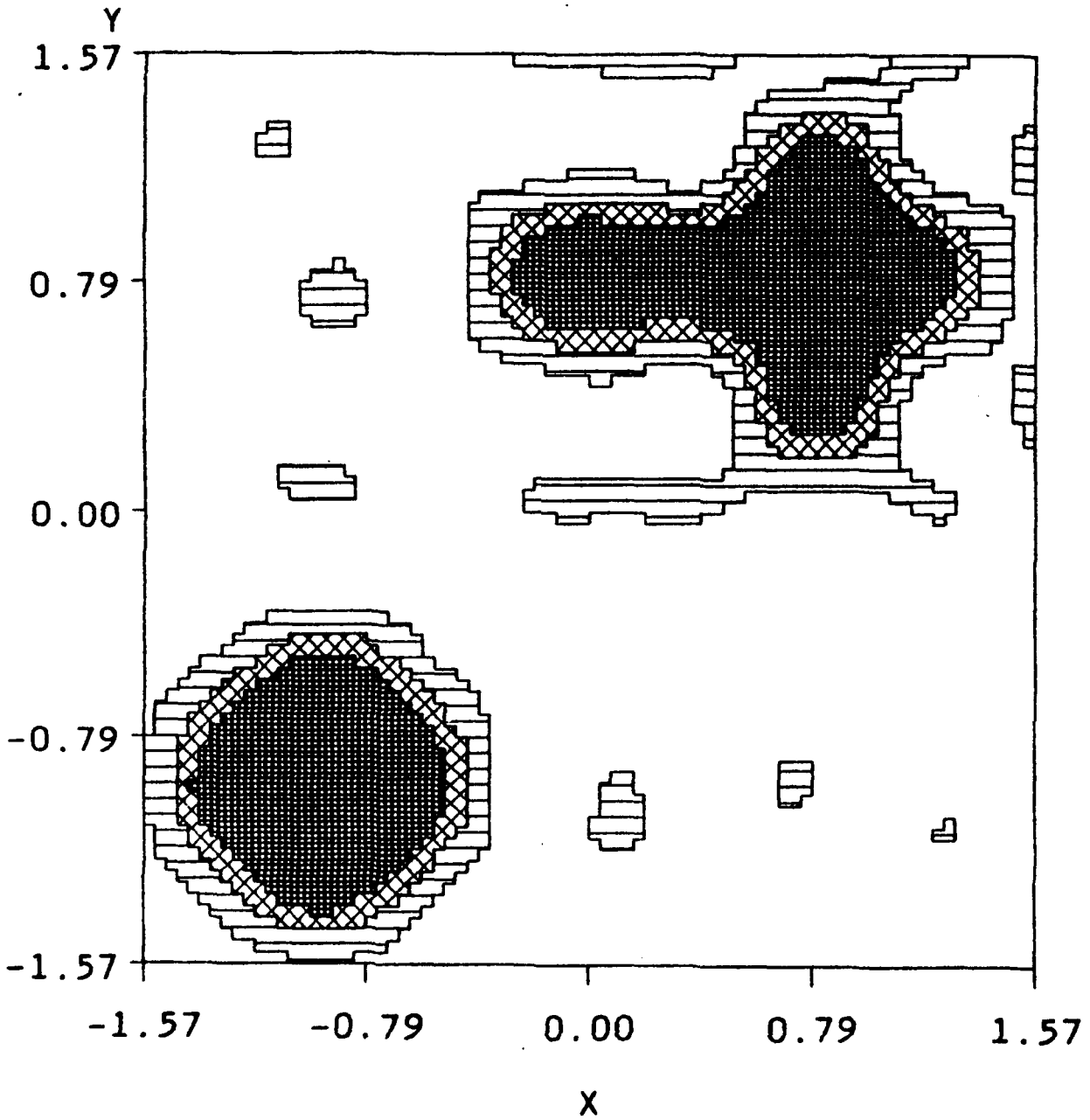

k = 10.1 m = 10

Test coefficient

Figure 2a

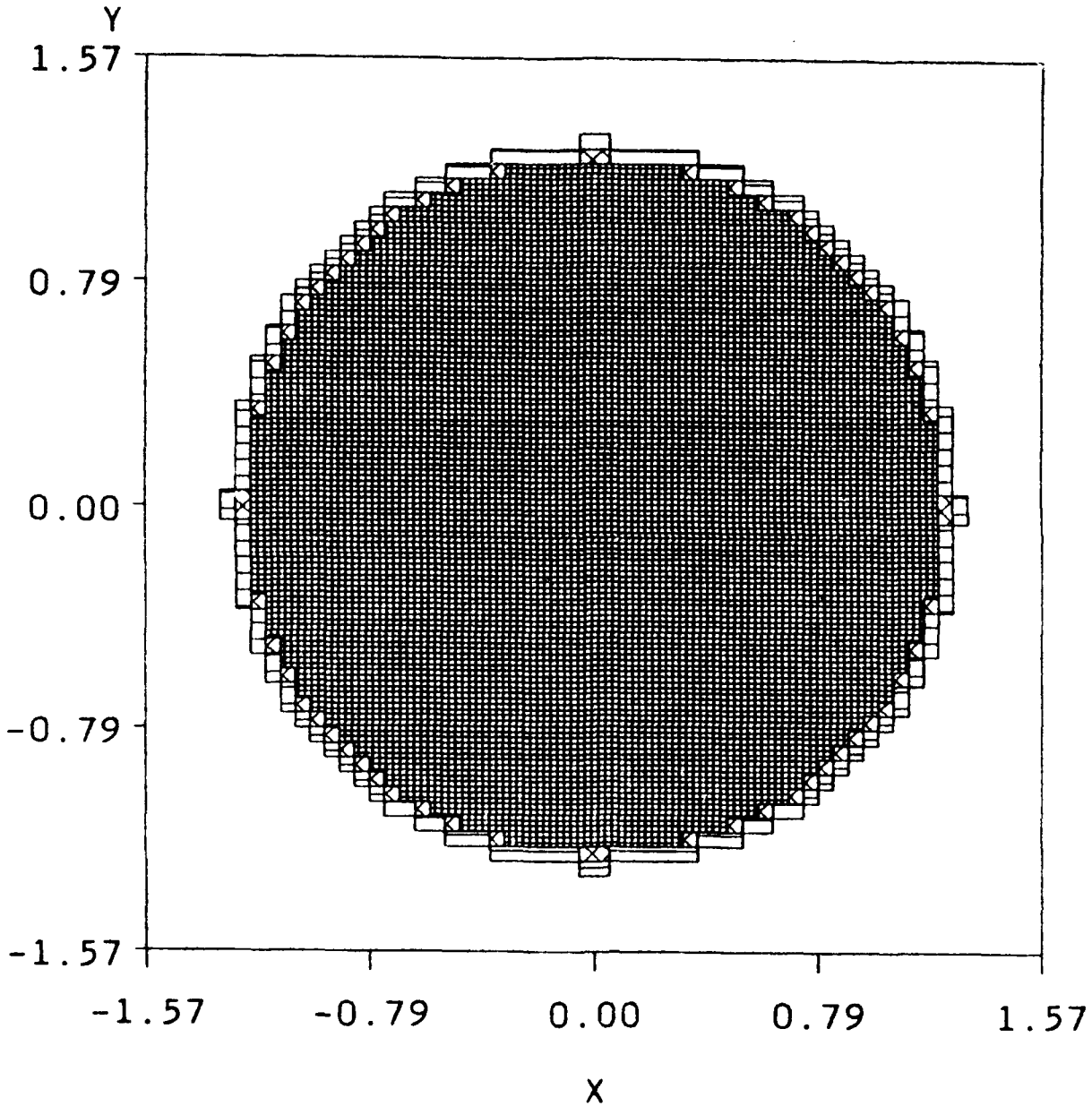

m = 7 a = 1.256637 α = 0.02 h = 0

Test coefficient

Figure 2b

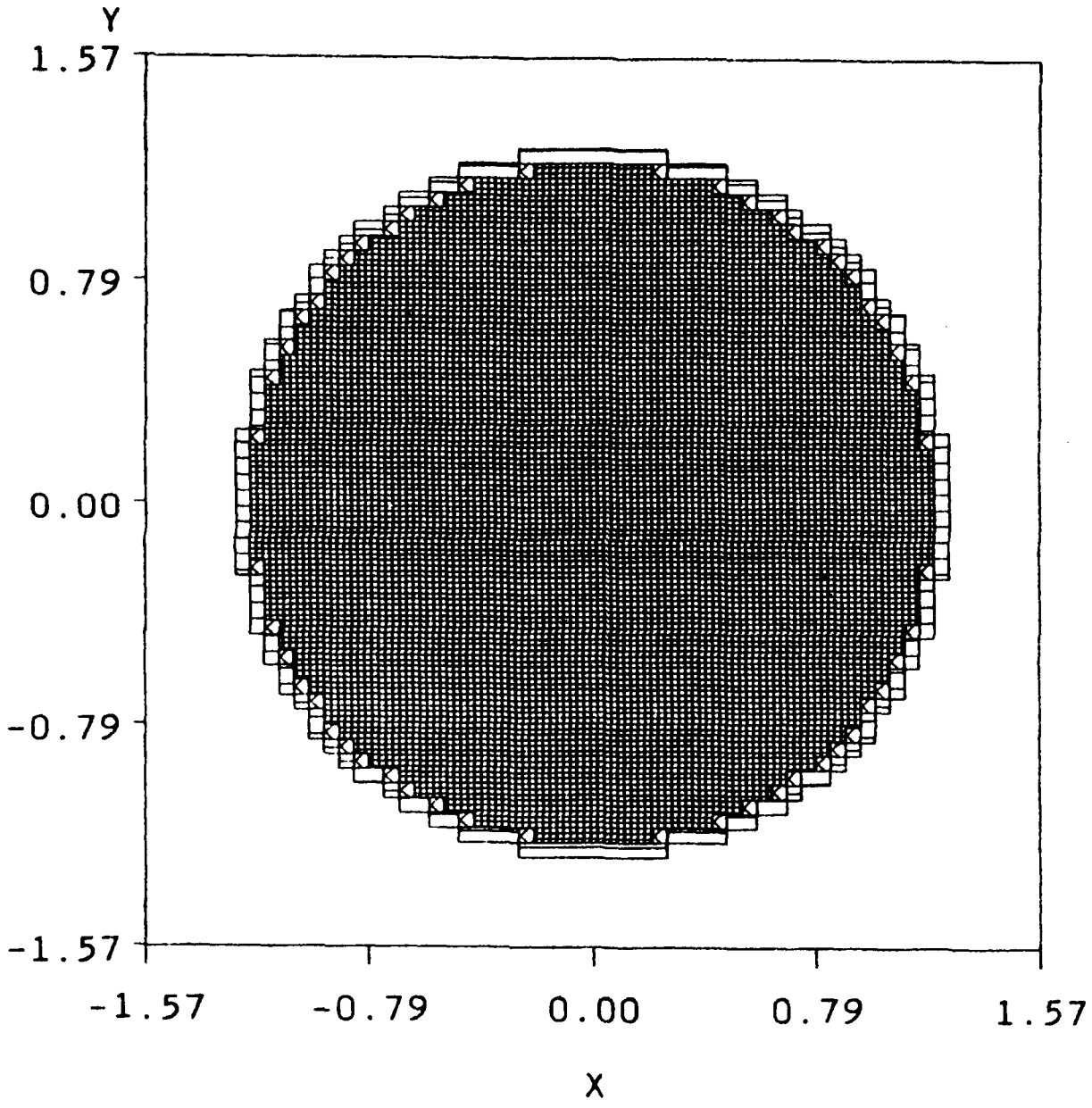

m = 7 a = 1.256637 α = 0.02 h = 0.261799

Figure 2c

Estimated coefficient

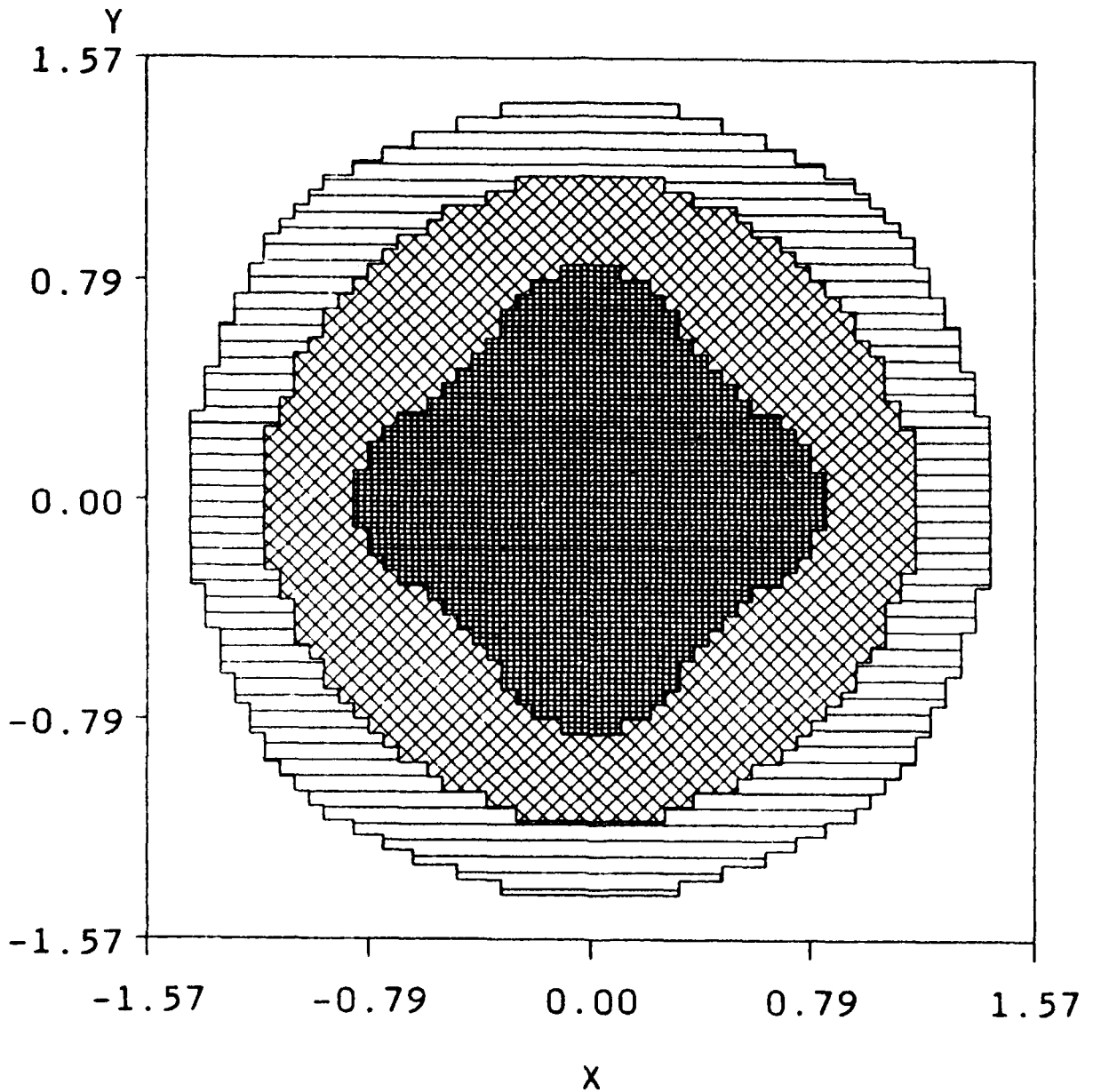

m = 7 a = 1.256637 α = 0.02 h = 0

Estimated coefficient

Figure 2d

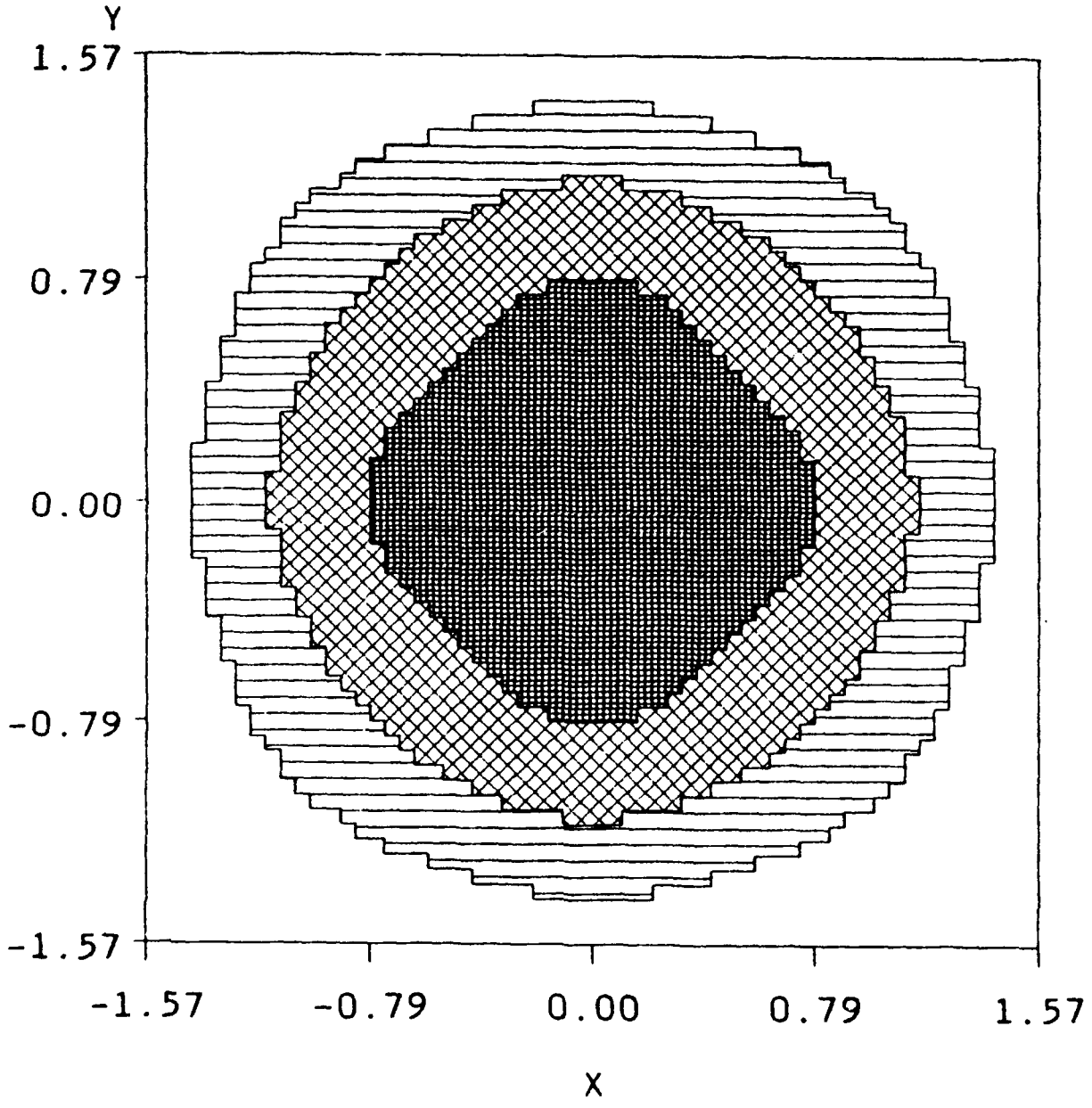

m = 7 a = 1.256637 α = 0.02 h = 0.261799

Figure 2e

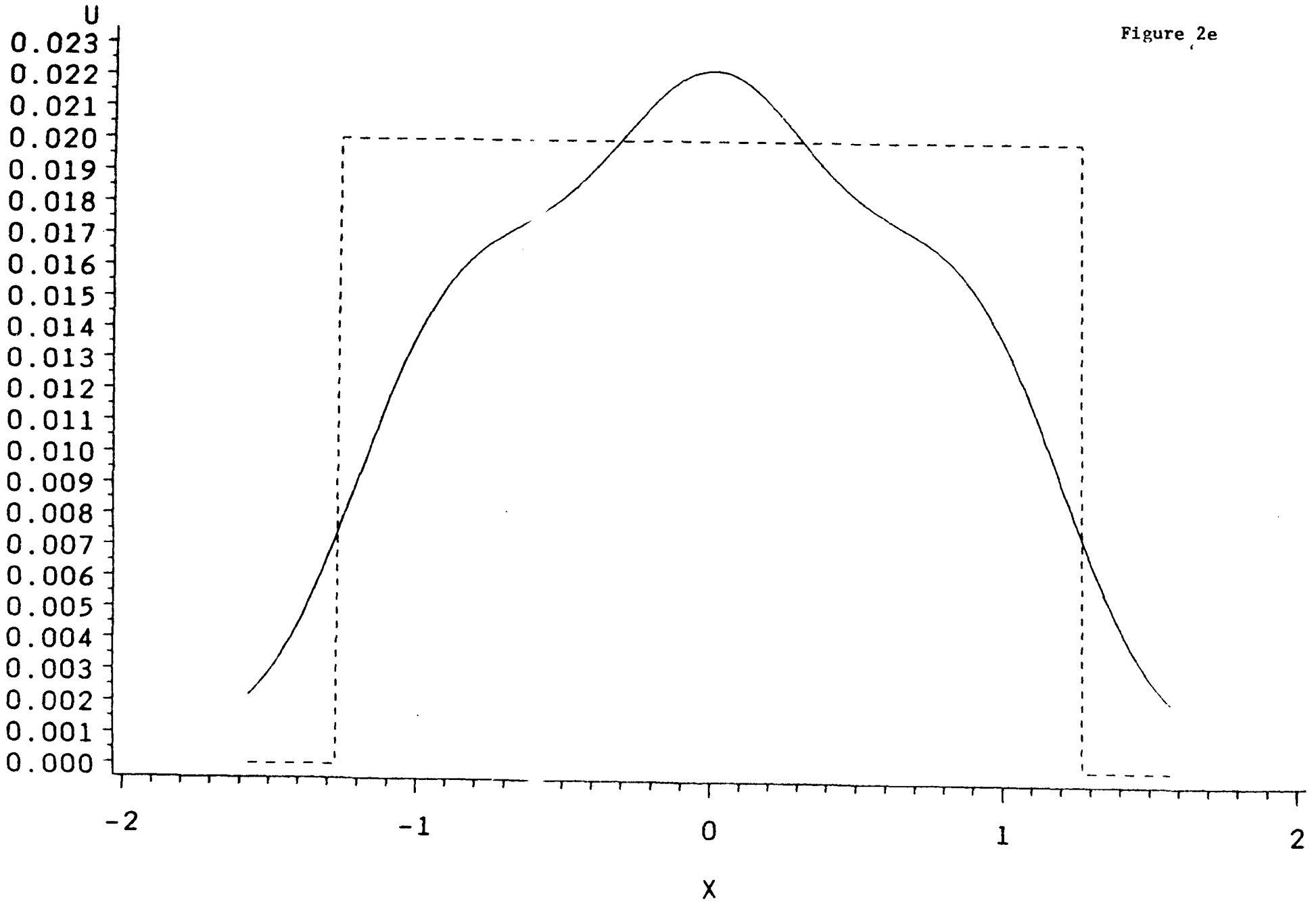

m = 7 a = 1.256637 α = 0.02

FIGURE 3

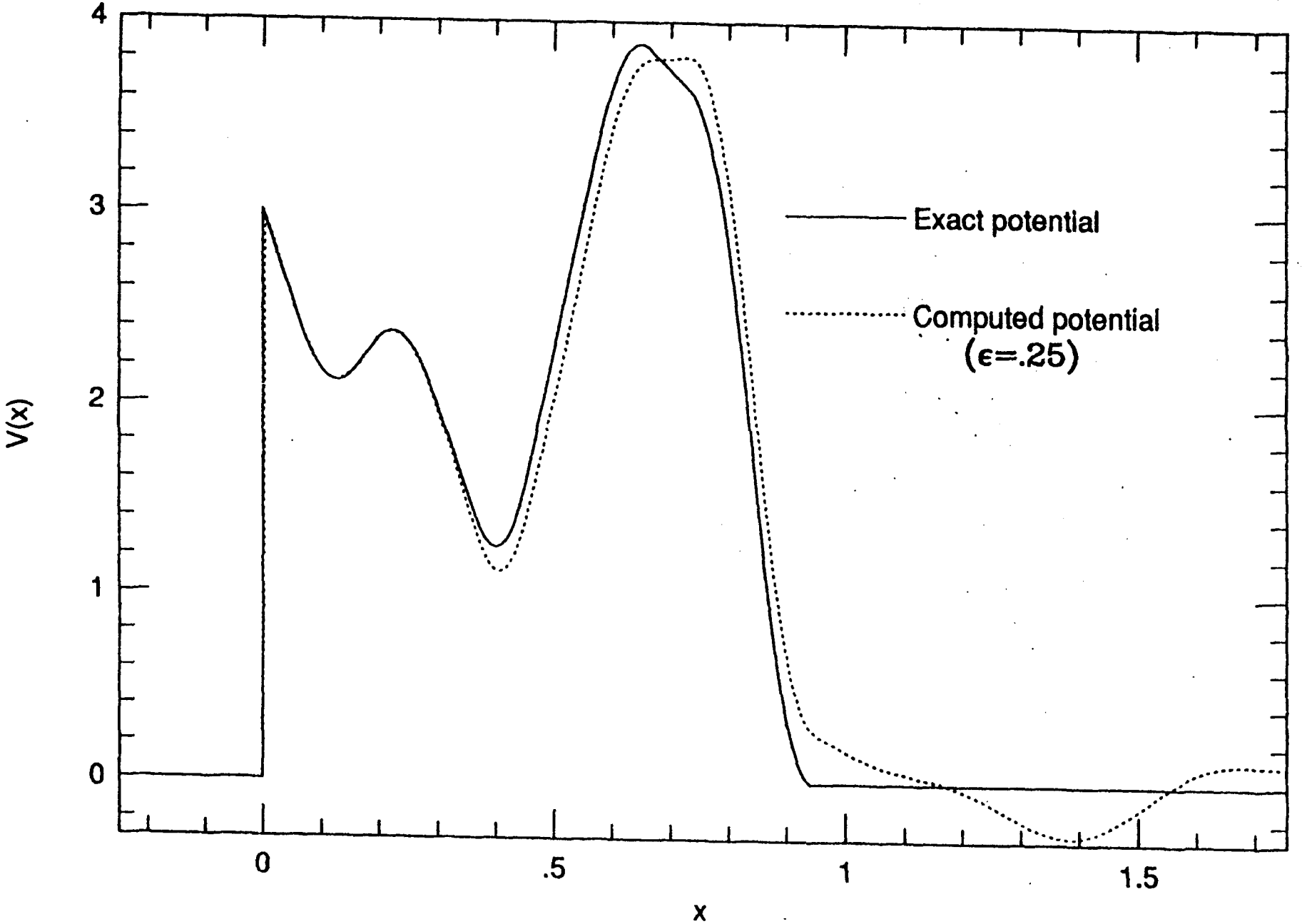

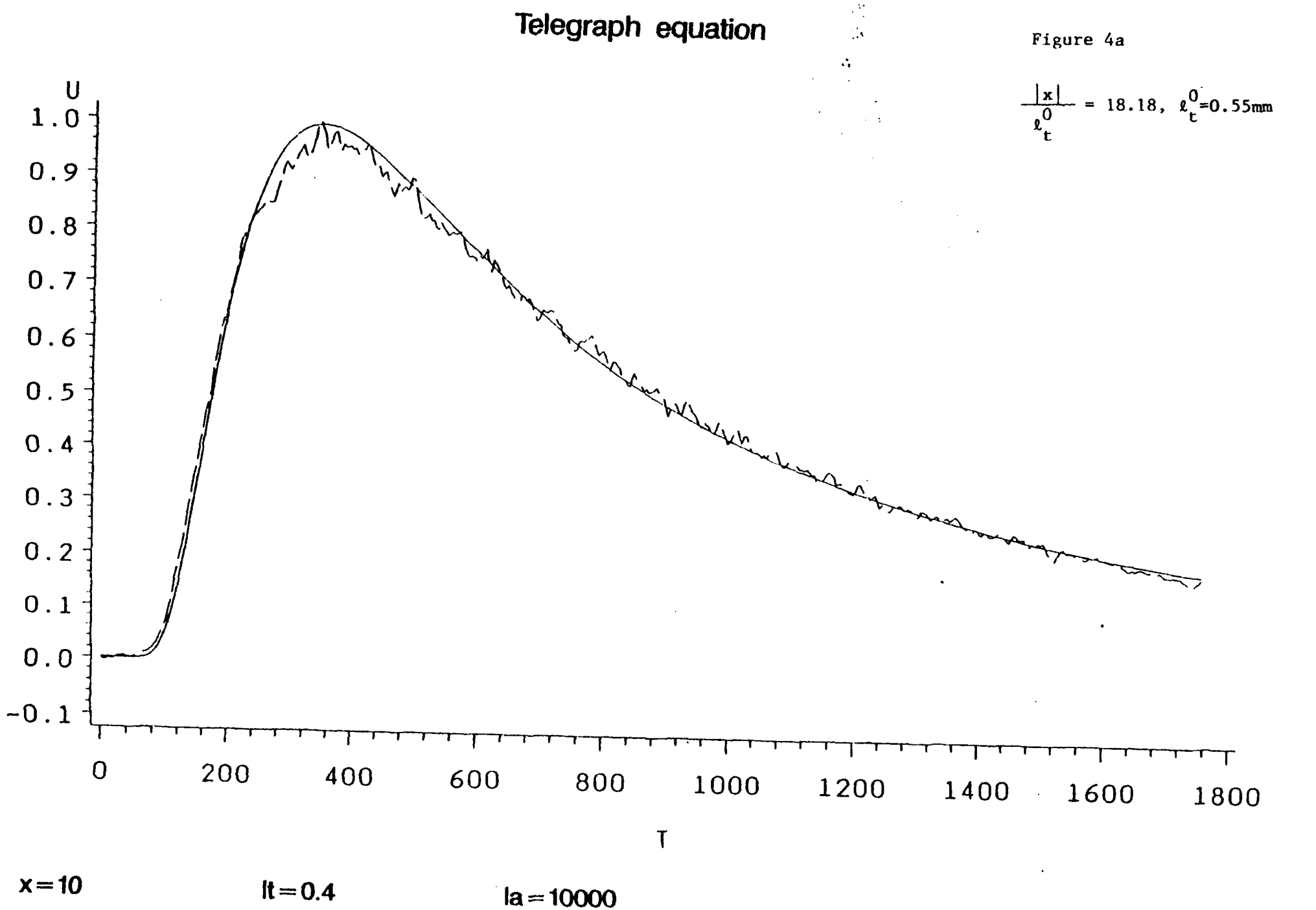

Figure 4a

$\frac{|x|}{\ell_t^0} = 18.18$, $\ell_t^0 = 0.55$mm

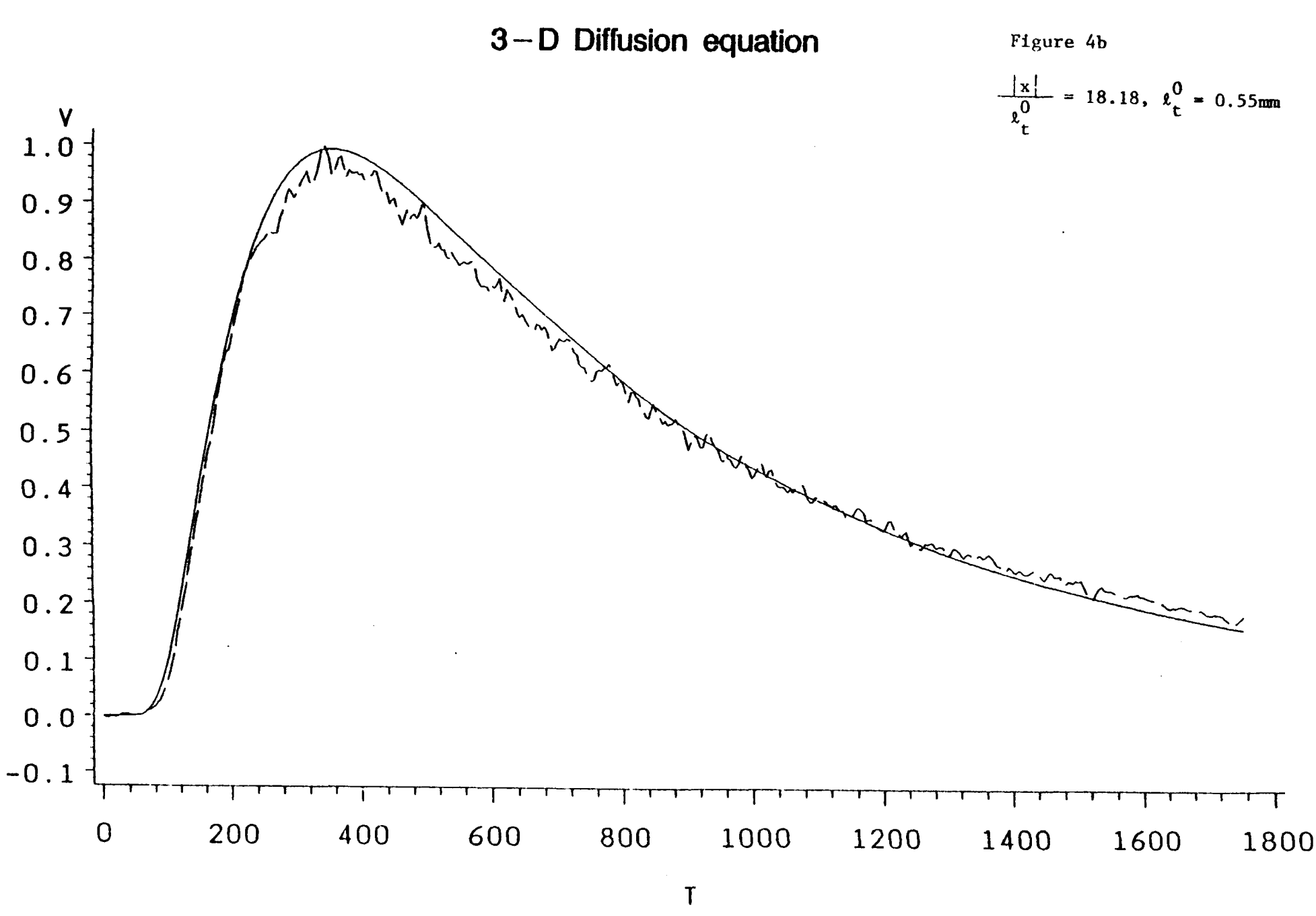

Figure 4b

$\frac{|x|}{\ell_t^0} = 18.18$, $\ell_t^0 = 0.55$mm

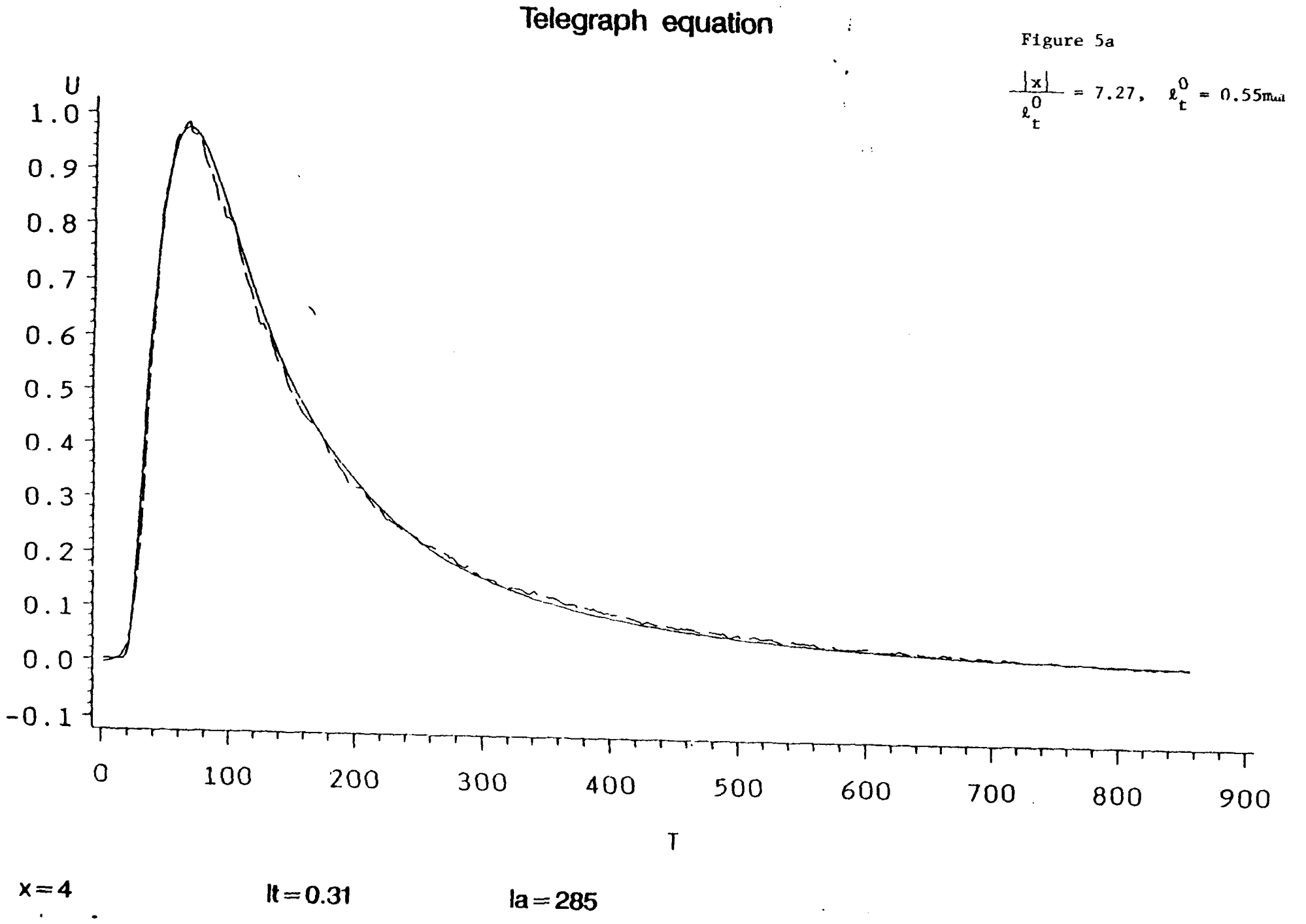

Figure 5a

$\frac{|x|}{\ell_t^0} = 7.27, \quad \ell_t^0 = 0.55 m_{ill}$

3 – D Diffusion equation

Figure 5b

$\frac{|x|}{\ell_t^0} = 7.27, \quad \ell_t^0 = 0.55\text{mm}$

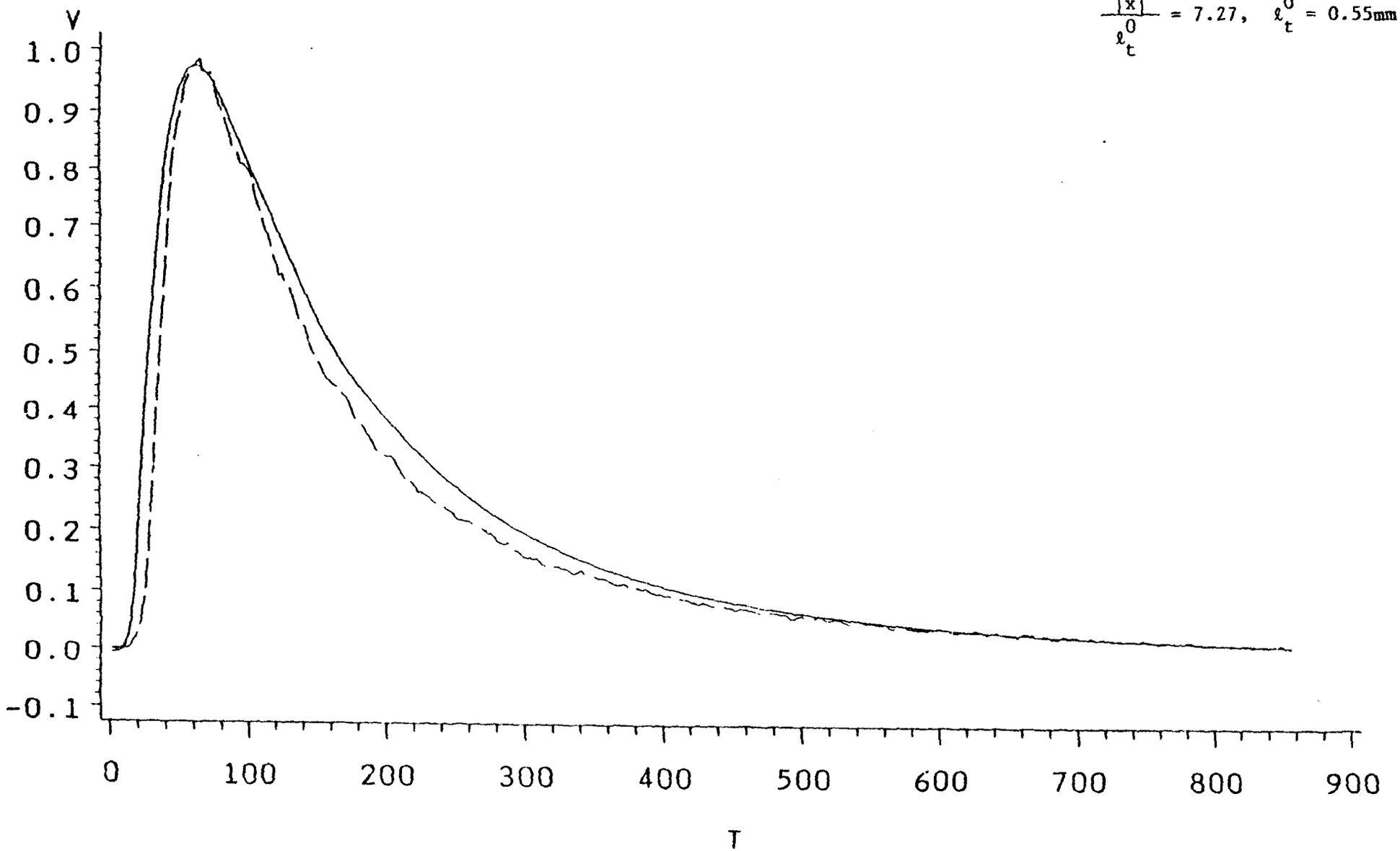

x=4 lt=0.52 la=100

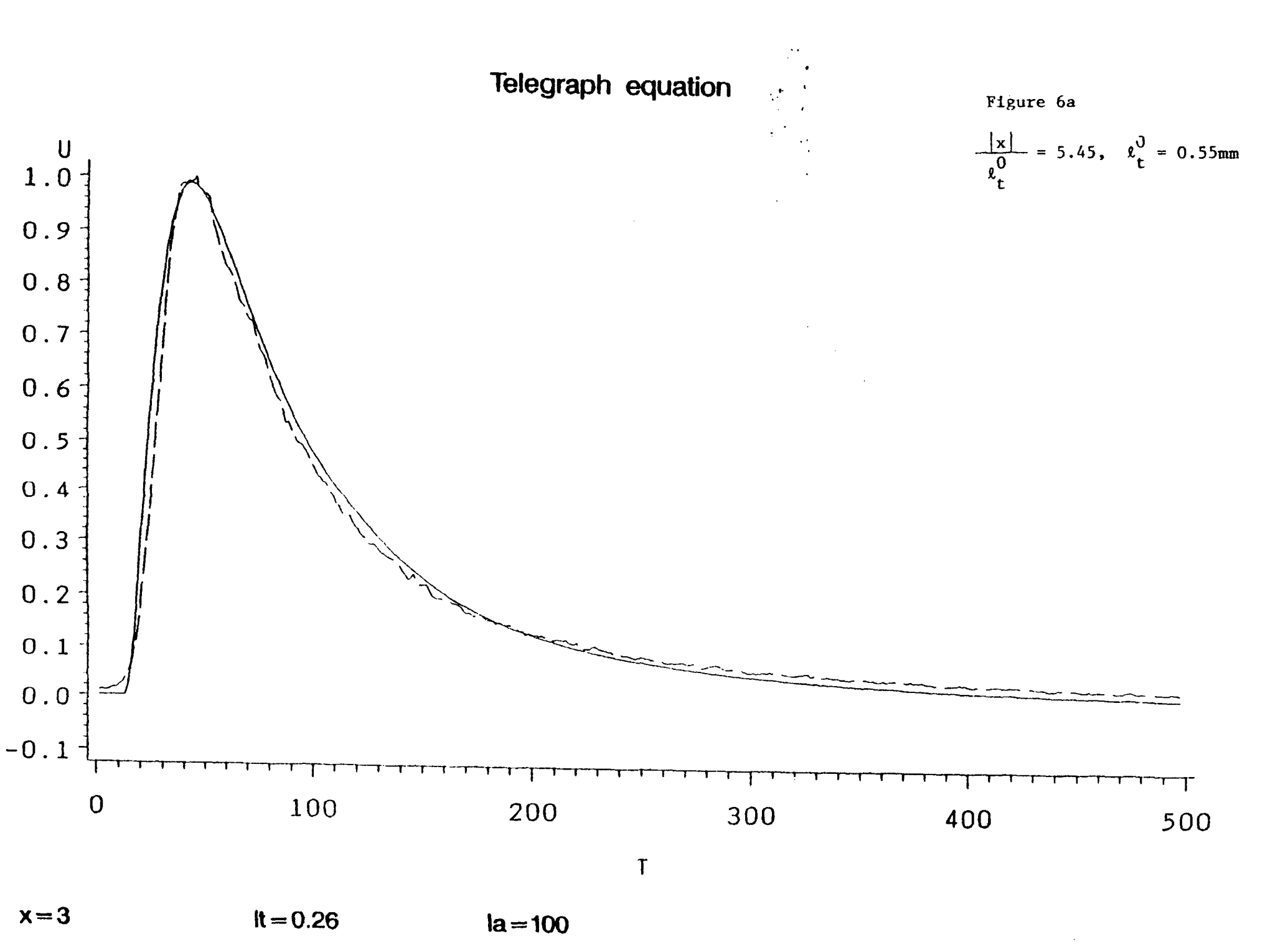

Figure 6a

$\frac{|x|}{\ell_t^0} = 5.45, \quad \ell_t^0 = 0.55\text{mm}$

3−D Diffusion equation

Figure 6b

$\frac{|x|}{\ell_t^0} = 5.45, \quad \ell_t^0 = 0.55\text{mm}$

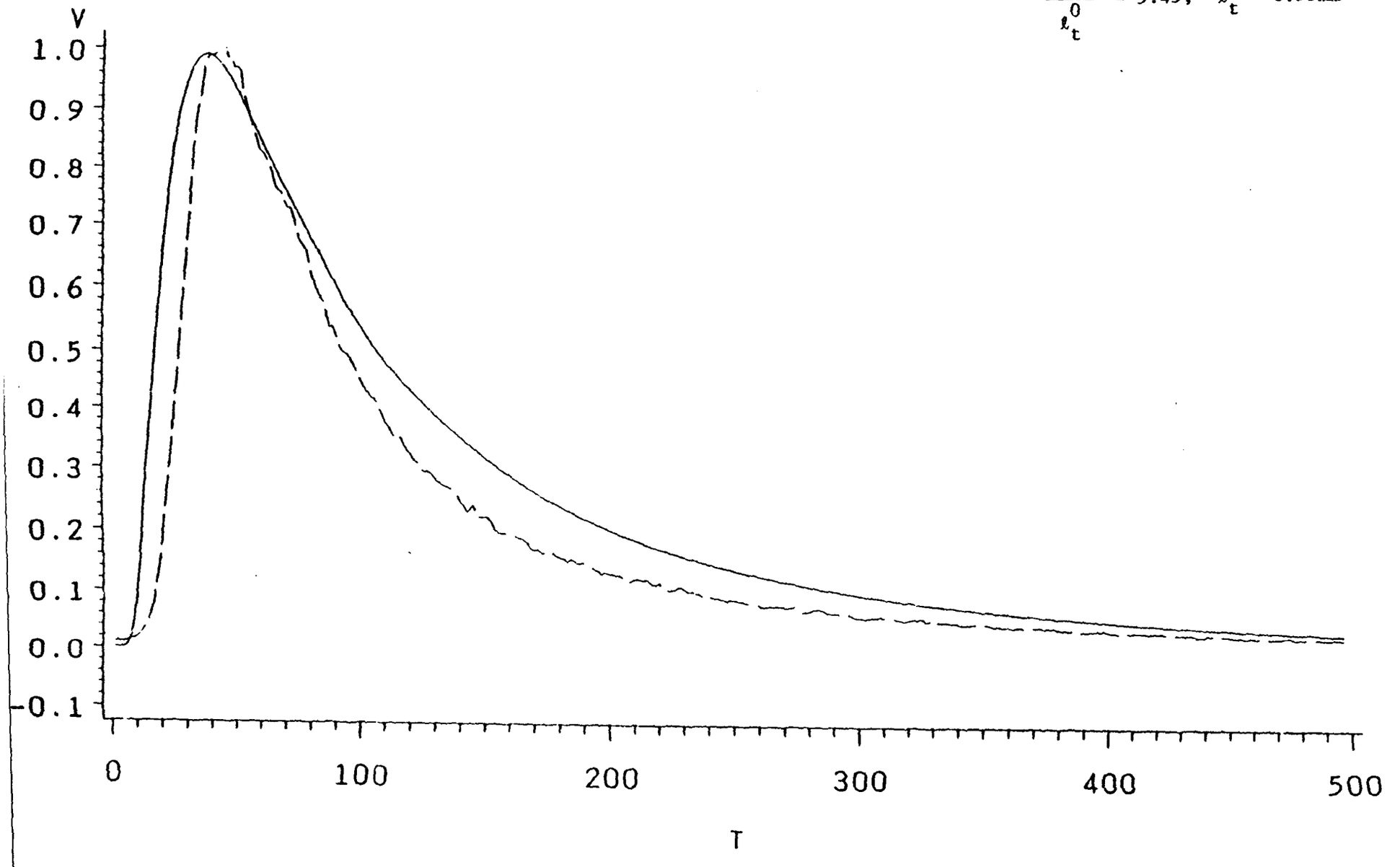

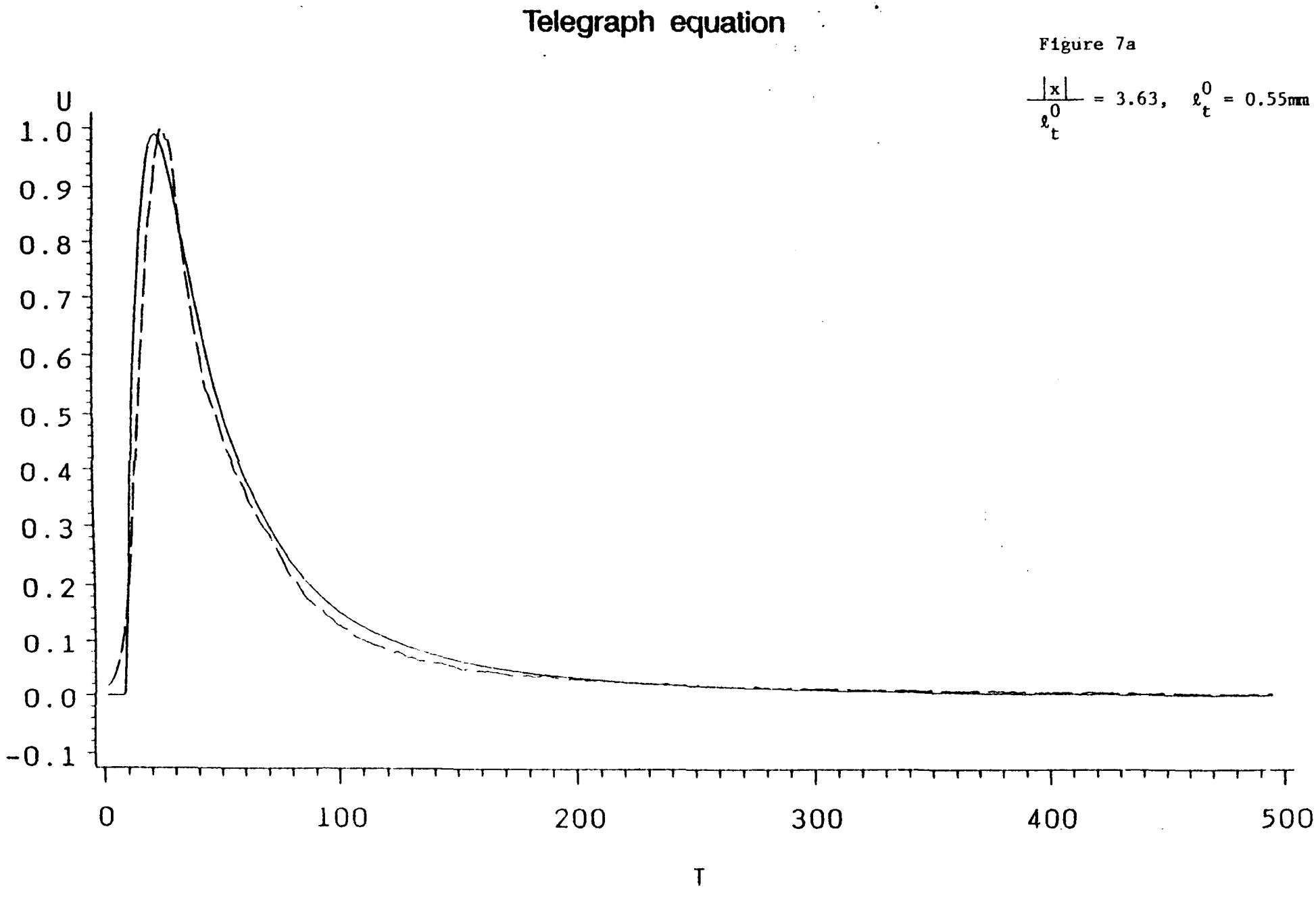

Figure 7a

$\frac{|x|}{\ell_t^0} = 3.63, \quad \ell_t^0 = 0.55\text{mm}$

3−D Diffusion equation

Figure 7b

$\frac{|x|}{\ell_t^0} = 3.63, \quad \ell_t^0 = 0.55\text{mm}$

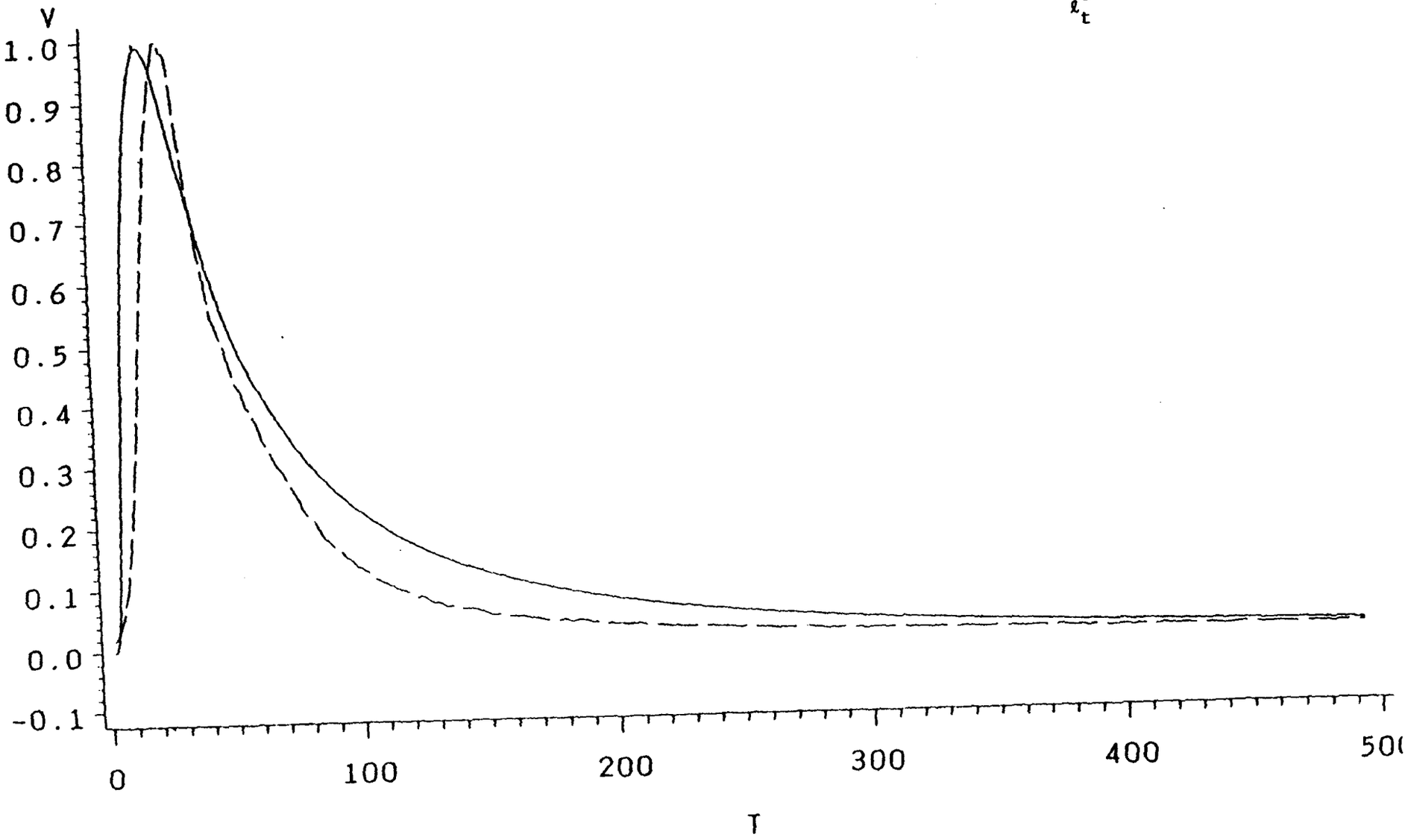

x=2 lt=0.48 la=100